

Curcumin regulates insulin pathways and glucose metabolism in the brains of APP^{swe}/PS1^{dE9} mice

International Journal of
Immunopathology and Pharmacology
2017, Vol. 30(1) 25–43
© The Author(s) 2017
Reprints and permissions:
sagepub.co.uk/journalsPermissions.nav
DOI: 10.1177/0394632016688025
journals.sagepub.com/home/iji


Pengwen Wang,^{1,2} Caixin Su,³ Huili Feng,^{1,2} Xiaopei Chen,^{1,4}
Yunfang Dong,^{1,2} Yingxue Rao,⁵ Ying Ren,^{1,2} Jinduo Yang,^{1,2}
Jing Shi,^{1,6} Jinzhou Tian,^{1,6} and Shucui Jiang³

Abstract

Recent studies have shown the therapeutic potential of curcumin in Alzheimer's disease (AD). In 2014, our lab found that curcumin reduced A β 40, A β 42 and A β -derived diffusible ligands in the mouse hippocampus, and improved learning and memory. However, the mechanisms underlying this biological effect are only partially known. There is considerable evidence in brain metabolism studies indicating that AD might be a brain-specific type of diabetes with progressive impairment of glucose utilisation and insulin signalling. We hypothesised that curcumin might target both the glucose metabolism and insulin signalling pathways. In this study, we monitored brain glucose metabolism in living APP^{swe}/PS1^{dE9} double transgenic mice using a micro-positron emission tomography (PET) technique. The study showed an improvement in cerebral glucose uptake in AD mice. For a more in-depth study, we used immunohistochemical (IHC) staining and western blot techniques to examine key factors in both glucose metabolism and brain insulin signalling pathways. The results showed that curcumin ameliorated the defective insulin signalling pathway by upregulating insulin-like growth factor (IGF)-1R, IRS-2, PI3K, p-PI3K, Akt and p-Akt protein expression while downregulating IR and IRS-1. Our study found that curcumin improved spatial learning and memory, at least in part, by increasing glucose metabolism and ameliorating the impaired insulin signalling pathways in the brain.

Keywords

Alzheimer's disease, APP^{swe}/PS1^{dE9} double transgenic mice, brain glucose metabolism, curcumin, IGF-1R, insulin signalling pathway

Date received: 16 August 2016; accepted: 6 December 2016

Introduction

Alzheimer's disease (AD) is the most common neurodegenerative disease among seniors.¹ Clinically,

AD patients display short-term memory impairment in the early stages and progressively develop

¹Key Laboratory of Chinese Internal Medicine of Ministry of Education and Beijing, Dongzhimen Hospital, Beijing University of Chinese Medicine (BUCM), Beijing, China

²Key Laboratory of Pharmacology of Dongzhimen Hospital (BUCM), State Administration of Traditional Chinese Medicine, Beijing, China

³Department of Surgery (Neurosurgery, Neurobiology) and Hamilton NeuroRestorative Group, McMaster University, Health Sciences Centre, Hamilton, ON, Canada

⁴Kaifeng Hospital of Traditional Chinese Medicine, Kaifeng, China

⁵Mizumori Lab, Department of Psychology, University of Washington, Seattle, WA, USA

⁶Beijing University of Chinese Medicine, BUCM Neurology Center, Dongzhimen Hospital, Beijing, China

Corresponding author:

Jinzhou Tian, Key Laboratory of Chinese Internal Medicine, Beijing University of Chinese Medicine, Ministry of Education, Beijing 100700, China.

Email: jztian@hotmail.com



other cognitive disabilities, personality changes and, ultimately, become completely dependent on others. Pathologically, AD is characterised by hallmarks such as senile plaques (SPs) and neurofibrillary tangles (NFTs).² The amyloid- β (A β) cascade has been a well-accepted hypothesis for AD.^{3,4} Recent studies in neuronal energy metabolism, however, suggest that AD could be conceptualised as a metabolic disease, with progressive impairment of the brain's capacity to utilise glucose and compromised response to insulin and insulin growth factor 1 (IGF-1).^{5,6}

The association between disruptions in glucose metabolism, insulin resistance and neuronal disorders has been well documented. In the early 1900s, it was noted that diabetes might also affect cognition.⁷ Other studies have confirmed that insulin may play an important role in the regulation of energy balance and glucose homeostasis, in association with other nutrition and adiposity signals.⁸⁻¹² It has been shown that energy metabolism impairment in neurons can trigger a cascade of pathological processes including oxidative stress, reactive oxygen generation, abnormal protein synthesis, cell membrane ion pump dysfunction, signal transduction impairment and neurotransmitter deficiency as well as abnormal degradation of A β precursor protein, A β accumulation and tau protein phosphorylation. These processes eventually lead to neuronal loss or death.^{8,9} Studies have indicated that AD shares some characteristics of diabetes such as dysfunction of insulin beta cell, glucose transporter (GLUT) changes¹⁰ and cholesterol and insulin concentration changes.^{11,12}

Although a connection between AD and diabetes was suggested a long time ago, only recently have studies have started to reveal the underlying mechanisms of brain insulin resistance and its contribution to the cognitive deficit in patients with AD. Reduced levels of insulin and insulin receptor (IR) molecules have been found in AD brains.¹³ In 2012, Talbot et al. demonstrated that, in AD cases without diabetes, the responses to insulin signalling in the IR/IRS-1/PI3K signalling pathway and responses to IGF-1 in the IGF-1R/IRS-2/PI3K signalling pathway were markedly reduced. Long-Smith et al. discovered that distinctive alterations in the localisation and distribution of IR molecules and increased levels of insulin receptor substrate (IRS)-1 phosphorylated at serine 616 (IRS-1 pS616), a key marker of insulin resistance, are

associated with A β plaque pathology in the frontal cortex of a mouse model of AD, APPSWE/PS1dE9.¹⁴ Treatment with liraglutide, an approved type 2 diabetes drug, was able to decrease IR aberrations in conjunction with a concomitant decrease in amyloid plaque load and levels of IRS-1 pS616.¹⁴

Collectively, these findings indicate that glucose intolerance and impaired insulin signalling may play a key role in the development of AD, and that targeting these underlying pathways may serve as a novel therapy and preventative measure for Alzheimer's-related dementia.

Curcumin is an active compound extracted from the root of the herb *Curcuma longa* and is the principal curcuminoid in the popular Indian spice, turmeric. A number of studies have demonstrated curcumin's therapeutic potential in cancer, diabetes and metabolic, autoimmune, infectious, neoplastic and neurodegenerative diseases.¹⁵⁻¹⁷ In vitro and in vivo studies have shown that curcumin can bind to A β and reduce existing SPs in AD.¹⁸⁻²¹ In our lab, using an APPSWE/PS1dE9 double transgenic mouse model, we found that three months after administration, curcumin significantly increases A β degradation enzymes insulin-degrading enzyme (IDE) and neprilysin and decreases γ -secretase PS2 subunit; however, the change in IDE is the most obvious. Curcumin also significantly decreases A β 40, A β 42 and aggregation of A β -derived diffusible ligands (ADDLs) expression in the hippocampus CA1 area, and spatial learning and memory ability were improved.²² Studies have shown that aggregation of ADDLs impairs the insulin signalling pathway in AD brains.²³⁻²⁵

Rosiglitazone (RSG), a medicine designed to treat type 2 diabetes, can improve AD patient cognitive function²⁶⁻²⁸ and was used as a positive control.

Given the link between a defective brain insulin signalling pathway and cognitive deficits in AD, it is reasonable to hypothesise that curcumin might improve learning and memory by ameliorating glucose intolerance and attenuating the defective insulin signalling pathway. This study is the cohort analysis from our 2014 publication. We used the same set of tissues from the mice which were examined for A β deposition and comparative cognitive testing.

In this study, we were able to monitor the brain glucose metabolism in living AD mice, using a micro-PET technique. The study showed that

curcumin improved cerebral glucose uptake in AD mice. We investigated key factors in both glucose metabolism and brain insulin signalling pathways including GLUT1, GLUT3, IR, insulin-like growth factor-1 receptor (IGF-1R), IRS-1, IRS-2, phosphatidylinositol-3-kinase (PI3K) and serine-threonine kinase (Akt) using IHC staining and western blot techniques. We anticipate that our study will provide a partial understanding of the mechanisms through which curcumin executes its therapeutic and preventative biological effects on AD.

Experimental procedures

Materials

Curcumin (cat. no. C1386) was purchased from Sigma-Aldrich. Rosiglitazone Maleate (cat. no. 09060108) was obtained from GlaxoSmithKline Ltd. Co. (Tianjin, China). The following primary antibodies were all purchased from Abcam (Hong Kong): GLUT1 (rabbit anti-mice, cat. no. ab652, diluted 1:250 for IHC staining and 1:500 for western blot analysis); GLUT3 (rabbit anti-mice, cat. no. ab41525, diluted 1:50 for IHC staining and 1:500 for western blot analysis); IR (rabbit anti-mice, cat. no. ab75998, diluted 1:50 for IHC staining and 1:100 for western blot analysis); IGF-1R (rabbit anti-mice, cat. no. ab39675, diluted 1:50 for IHC staining and 1:500 for western blot analysis); IRS-1 (rabbit anti-mice, cat. no. ab52167, diluted 1:50 for IHC staining and 1:500 for western blot analysis); PI3K (rabbit anti-mice, cat. no. ab74136, diluted 1:50 for IHC staining and 1:500 for western blot analysis); p-PI3K (rabbit anti-mice, cat. no. ab61801, diluted 1:50 for IHC staining and 1:500 for western blot analysis), Akt (rabbit anti-mice, cat. no. ab8805, diluted 1:200 for IHC staining and 1:500 for western blot analysis); and p-Akt (rabbit anti-mice, cat. no. ab38513, diluted 1:50 for IHC staining and 1:2000 for western blot analysis). The Strept Actividin-Biotin Complex and 3,3'-diaminobenzidine (DAB) development kits were obtained from Wuhan Boster Bio-engineering Ltd. Co. (Wuhan, China). The ECL western blot substrate kit was purchased from Shangbo Beijing Biomedical Technology (cat. no. WBKLS 0100). The PVDF membrane was purchased from Millipore (cat. no. IDVH 00010). All other chemicals were purchased from the Beijing Huanyataike Biomedical Technology Company.

The Mini-PROTEAN® 3 gel electrophoresis instrument was purchased from Bio-Rad. The PET radiotracer 18F-FDG (fluodeoxyglucose) was provided by the PET Department of the People's Liberation Army (PLA) General Hospital. The PET imaging system (Inveon PET//computed tomography [CT]) was purchased from Siemens, Germany. The system detector material was lutetium oxyorthosilicate crystal. It provides an axial field of vision of 12.7 cm and delivers less than 1.7 mm axial spatial resolution at 1 cm from the centre of the field of vision, with a time resolution less than 1.5 ns. A CT scan was applied for attenuation correction. The CT correction scan time was about 5 min; the PET scan time was 10 min. Images were analysed by the Motic Digital Medical Image Analysis System 6.0 (China).

Animals

The APP^{swe}/PS1^{dE9} double transgenic mice and wild-type C57/BL6J mice were purchased from the Institute of Laboratory Animal Science at the Chinese Academy of Medical Sciences (SCXK [Beijing] 2009-0004) and were housed in the Barrier Environment Animal Lab at the Key Laboratory of Pharmacology of Dongzhimen Hospital which is affiliated with Beijing University of Chinese Medicine (BUCM) (SYXK [Beijing] 2009-0028). All experiments were performed in compliance with Beijing's regulations and guidelines for the use of animals in research and had been approved by the Animal Research Ethics Board of Dongzhimen Hospital. To represent the whole population, both male and female mice (1:1) were chosen. They were maintained in a temperature-controlled vivarium on a 12:12 h light:dark cycle with food and tap water freely available. After spending one week acclimating to the new environment, treatments were started when the mice were three months old. They were randomly divided into six groups, with 12 in each group. Wild-type C57/BL6J mice were used as a normal control (Wild). APP^{swe}/PS1^{dE9} double transgenic mice were used in all other groups: in the control group (Control), a vehicle was used for treatment. In the positive control group, 10 mg/kg/day RSG was used for treatment. The following doses were used for curcumin treatment: low dose curcumin group (LDC): 100 mg/kg/day; medium dose curcumin group (MDC): 200 mg/kg/day; high dose curcumin group (HDC): 400 mg/kg/day.

Gavage

Curcumin and RSG were dissolved in 0.5% sodium carboxymethyl cellulose (CMC) and gavaged to mice at 0.1 mL/10 g body weight for three months. An equivalent amount of 0.5% CMC was used for the Wild and the Control groups.

Micro-PET scan

After three months of treatment, three mice from each of the Wild, Control and MDC groups were randomly chosen for micro-PET scanning. Blood was taken to ensure that glucose readings were in the normal range (7–10.1 mmol/L). Mice were fasted for 6 h prior to the PET scan. After being anaesthetised with 2% isoflurane, mice were injected with 14.8–16.5 MBq radiotracer ¹⁸F-FDG through the tail vein. A 10-min prone acquisition scan was performed 45 min after injection. Mice were maintained under isoflurane anaesthesia for the duration of the procedure. Dynamic micro-PET image was reconstructed by using a filtered-back projection algorithm and a CT attenuation correction was applied. The acquisition rate of the dynamic PET image was 30 frames/s. Three-dimensional regions of interest (ROI) were manually drawn for the brain (excluding cerebellum) on horizontal, sagittal and coronal planes, and average radioactivity per gram of tissue was calculated in the ROI. The mean and maximum activities were recorded for the entire ROI. The percentage injected dose (ID) per gram (% ID/g) was calculated as follows: % ID/g = ROI activity divided by injected dose and per gram multiplied by 100%.

Tissue preparation

After the behaviour test, six mice per group were sacrificed for IHC analysis. To summarise, they were deeply anaesthetised with 10% chloral hydrate (400 mg/kg body weight, i.p.) and were quickly cardio-perfused with 50 mL 0.9% physiological saline, followed by 60 mL of 4% paraformaldehyde. After decapitation, brains were removed and incubated in the same fixative solution until they sank to the bottom of the jar. After that, the fixative solution was changed one more time and paraffin embedding was performed. Serial coronal sections of the hippocampal CA1 region were cut at 4 µm intervals. Five consecutive sections of the hippocampal CA1 region from each mouse were

analysed under 20× magnification to count the number of positively stained neurons. Photographs were taken and analysed with Motic Med 6.0 Image software. Data are expressed as the number of positive stained cells per group.

A separate set of animals (n = 6/group) were killed by decapitation. Hippocampal tissue was dissociated immediately on ice, placed in cryovials and stored in liquid nitrogen until needed for western blot analysis.

Western blot analysis

Western blot procedures were performed as described previously.²⁹ Hippocampal tissue was put into whole cell lysis buffer (50 mL/g tissue) with the following composition: 50 mM Tris-HCl (pH 7.5), 0.1 mM EDTA, 0.1 mM EGTA, 1 mM DTT, 0.2% NP40, 5 mg/L leupeptin, 2 mL/L aprotinin and 50 mg/L soybean trypsin inhibitor. Cell lysates were homogenised and centrifuged at 12,000 r.p.m. for 5 min at 4°C. Proteins were quantified by bicinchoninic acid assay.³⁰ Protein samples were heated in boiling water for 5 min and separated with SDS-PAGE under 120 V. They were subsequently transferred electrophoretically to a polyvinylidene difluoride membrane by applying a 200-mA current at 4°C for 2 h. The membrane was pre-stained with Ponceau stain and was then washed three times for 5 min with phosphate buffered saline-Tween 20 (PBST). After blocking with 5% skimmed milk for 3 h, the membrane was hybridised with primary antibodies²⁹ overnight at 4°C. They were then rinsed with PBST for 3–5 min, incubated with horseradish peroxidase (HRP)-conjugated IgG secondary antibody (1:5000, Jackson ImmunoResearch, Beijing, China) for 1 h and examined by enhanced chemiluminescence (Beijing Dingguo Biotechnology Inc., Beijing, China) for 3 min. After stripping, the same membrane was then used to detect β-actin (1:5000). The protein bands were quantified with NIH Image J software and β-actin was used as the internal control.

Immunohistochemical staining and quantification

Details of the IHC procedures have been described elsewhere.³¹ Briefly, paraffin sections underwent deparaffinisation in a 56°C oven for 1

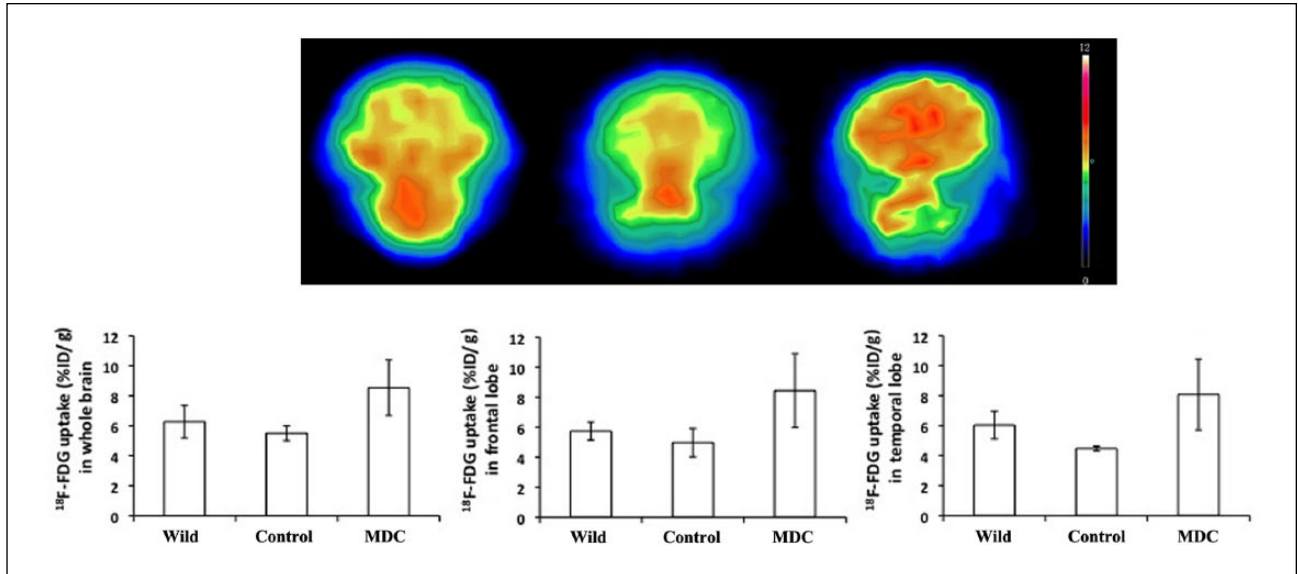


Figure 1. Glucose metabolism analysed by PET. The same colour code was used for all images, with high to low glucose metabolism shown from top to bottom. The results showed that the average glucose metabolism in the MDC group was higher than that of both the Wild and the Control groups. The ^{18}F -FDG uptake ratio in different areas of the mice brain, including whole brain, frontal lobe and temporal lobe, was analysed using PET. In all tested locations, the ^{18}F -FDG uptake ratio in the MDC group was significantly higher than in the Control group ($P < 0.05$, $n = 3$).

h, then were submersed in p-xylene 1 and p-xylene 2 for 20 min, followed by sequential washes with 100%, 95%, 80% and 70% alcohol for 3–5 min each respectively. Finally, the slices rested in distilled water for 5 min. Subsequently, sections were incubated in 3% H_2O_2 (hydrogen peroxide) in absolute methanol for 15 min and were washed with PBST for 5 min. The sections were then treated with 5% goat serum for 30 min on an orbital shaker to block non-specific antibody binding. Overnight incubation with primary antibody in humidified boxes at 4°C ensued. The following day, sections were again rinsed three times in PBST (5 min/time) and were incubated with reagent 1 (Polymer Helper, Ready-to-use PV-9001 or PV-9002, ZSGB-BIO, Beijing, China) at 37°C for 1 h. Afterward, they were rinsed three more times with PBST for 3–5 min/time and then were incubated with HRP-reagent 2 (poly-HRP anti-Rabbit IgG or anti-Mouse IgG, Ready-to-use PV-9001 or PV-9002, ZSGB-BIO, Beijing, China) at 37°C for 1 h. After a final set of 3–5 min rinses with PBST, staining was developed with 3,3'-diaminobenzidine (DAB) substrate for 5–10 min. Sections were mounted, dehydrated, cover slipped and examined under a microscope. The primary antibodies used were described earlier in the 'Materials' section.

To verify the specificity of antibodies, negative controls with rabbit serum instead of primary antibodies were included in each test. Two sections per mice were used for each staining, for a total of 12 sections from each group. Positively stained neurons in the hippocampal CA1 region were counted at $10\times$ magnification and photographs were taken and analysed with Motic Med 6.0 Image software. Data are expressed as the number of positively stained cells per group.

Statistical analysis

All data were analysed with SPSS 15.0 software and presented as mean \pm standard deviation (SD). One-way analysis of variance (ANOVA) and non-parametric tests were used for analysis and post-hoc comparisons were made using a least-significant difference test. Data were considered statistically significant at $P < 0.05$.

Results

PET analysis

Figure 1 shows the glucose metabolism as analysed by PET. The same colour code was used for all images. The images indicate that three months after treatment, the average glucose metabolism of

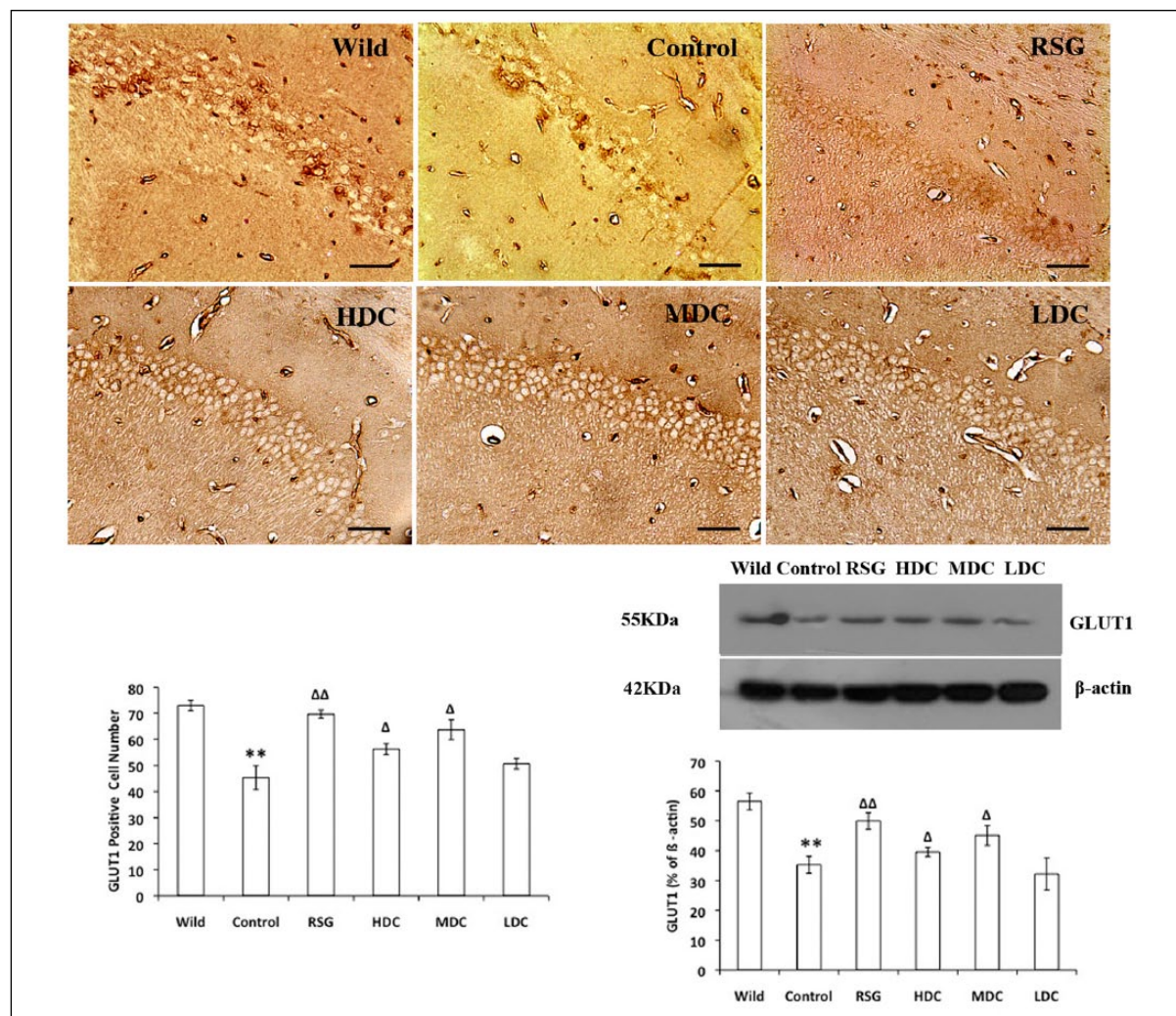


Figure 2. Effect of curcumin on GLUT1 expression in the hippocampal CA1 region. The top panel shows the GLUT1 IHC staining images with the yellow-tan positive staining of GLUT1 localised in the cytomembrane of the hippocampal CA1 region, as indicated in the big circular and oval-shaped cell bodies. Quantification results of the IHC staining are shown on the bottom left panel. The bottom right panel shows the western blot images and quantification results. Both IHC and western blot testing show that there is significantly more GLUT1 protein expression in the RSG ($P < 0.01$), HDC and MDC groups ($P < 0.05$) than in the Control group. *indicates the difference from wild-type mice; ** indicates significance of $p < 0.01$ and Δ indicates significance of $p < 0.05$; $\Delta\Delta$ indicates significance of $p < 0.01$ and Δ indicates significance of $p < 0.05$. Scale Bar=50 μm .

the mice in the MDC group was higher than that of the glucose metabolism of the mice in the Wild and Control groups.

We then analysed the ^{18}F -FDG uptake ratio in different areas, including the whole brain, frontal lobe and temporal lobe. In all the locations we tested, the ^{18}F -FDG uptake ratio in the MDC group was significantly higher than in the Wild and Control groups (Figure 1; $P < 0.05$, $n = 3$).

Effects of curcumin on GLUT1 expression in the hippocampal CA1 region

IHC staining showed that the yellow-tan positive staining of GLUT1 localised in the cytomembrane of

the hippocampal CA1 region, with big circular or oval-shaped cell bodies (Figure 2). Quantification results showed that, in contrast to the wild-type mice, the number of GLUT1 positively stained cells was significantly lower in the Control group ($P < 0.01$). Compared with the Control group, the number of positively stained cells was significantly higher in the RSG ($P < 0.01$), HDC and MDC groups ($P < 0.05$).

Western blot analysis showed that GLUT1 expression was significantly reduced in the Control group compared with the Wild group ($P < 0.01$). RSG, MDC and HDC treatments, however, significantly increased protein expression of GLUT1 ($P < 0.01$ for RSG and $P < 0.05$ for MDC and HDC) compared with the Control group (Figure 2).

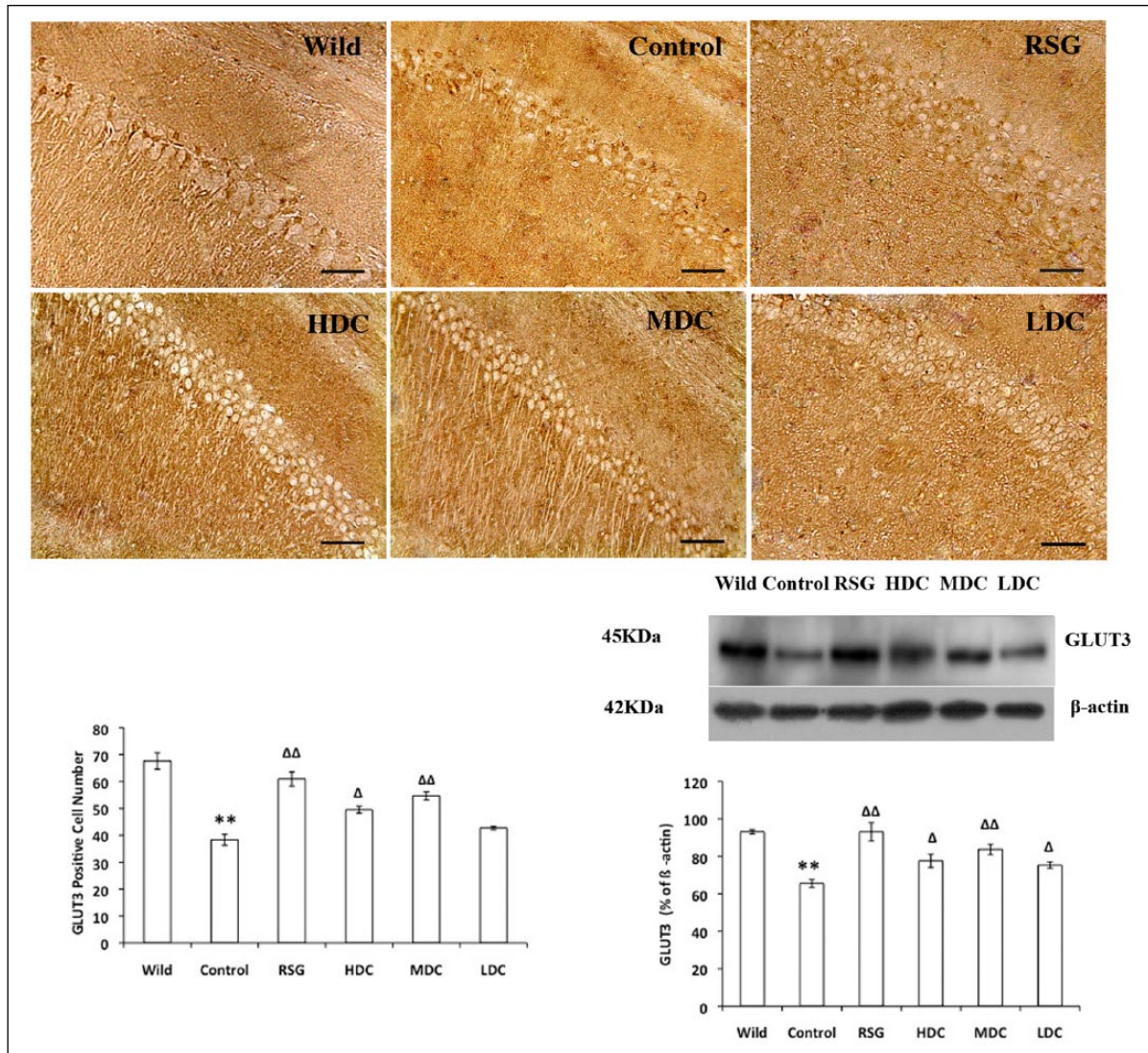


Figure 3. Effect of curcumin on GLUT3 expression in the hippocampal CA1 region. Both the IHC testing and western blot analysis show that HDC ($P < 0.05$), RSG and MDC ($P < 0.01$) treatment significantly improved GLUT3 expression compared with that of vehicle treatment in the Control group. Western blot analysis of LDC treatment showed a significant ($P < 0.05$) improvement in GLUT3 expression compared with that of the Control group.

Effects of curcumin on GLUT3 expression in the hippocampal CA1 region

The results of the GLUT3 staining were similar to those of the GLUT1 staining. Compared with the Wild group, there were fewer GLUT3-positive cells in the mice in the Control group ($P < 0.01$). The number of positively stained cells in the HDC group was significantly ($P < 0.05$) higher than in the Control group. The difference was even more significant in the RSG and MDC treatment groups ($P < 0.01$) (Figure 3).

Western blot analysis showed that GLUT3 expression was significantly lower in the transgenic

mice (Control) compared with the Wild group ($P < 0.01$). HDC and LDC treatment significantly increased protein expression of GLUT3 compared with the Control group ($P < 0.05$). The difference in GLUT3 expression between the Control group and RSG and MDC treatment groups was even more significant ($P < 0.01$) (Figure 3).

Effects of curcumin on IR expression in the hippocampal CA1 region

IHC staining showed that, in the hippocampal CA1 region, IR antibody positively stained the cytomembrane and cytoplasmic parts; the staining was most

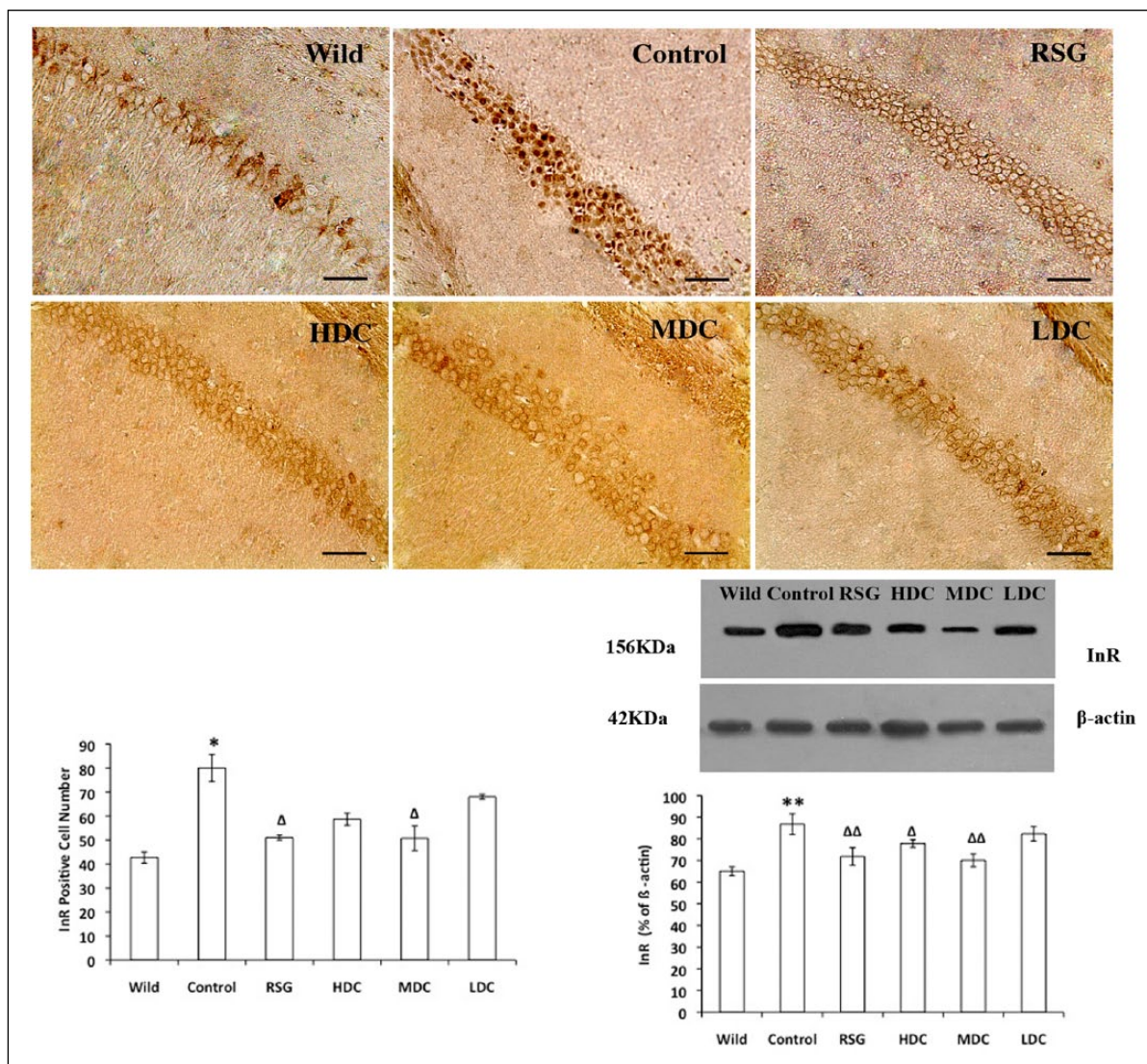


Figure 4. Effect of curcumin on IR expression in the hippocampal CA1 region. IHC analysis revealed that curcumin treatment showed a significant difference in the RSG and MDC groups ($P < 0.05$) compared with the Control group. However, western blot analysis indicated a significant difference between the RSG and MDC groups ($P < 0.01$) and HDC group ($P < 0.05$) compared with the Control group.

obvious in the Control group. Quantification showed that the number of IR positive cells in the Control group was significantly higher than in the Wild group ($P < 0.05$). Compared with the Control group, the numbers of positively stained cells in the RSG and MDC groups were significantly lower ($P < 0.05$) (Figure 4).

Western blot analysis showed that there was more IR expression in the Control group than in the Wild group ($P < 0.01$). Compared with the Control group, the bands from all treatment groups were narrower. Quantification showed that IR protein expression was significantly reduced in the HDC group ($P < 0.05$) compared with the Control

group; the difference was particularly significant ($P < 0.01$) in the RSG and MDC groups (Figure 4).

Effects of curcumin on IGF-1R expression in the hippocampal CA1 region

IHC staining revealed that there were significantly less IGF-1R positively stained cells in the Control group than in the Wild group ($P < 0.01$). RSG and curcumin treatments reversed this trend. Quantification results showed that the RSG, HDC and MDC groups contained significantly more IGF-1R positively stained cells than the Control group ($P < 0.01$) (Figure 5).

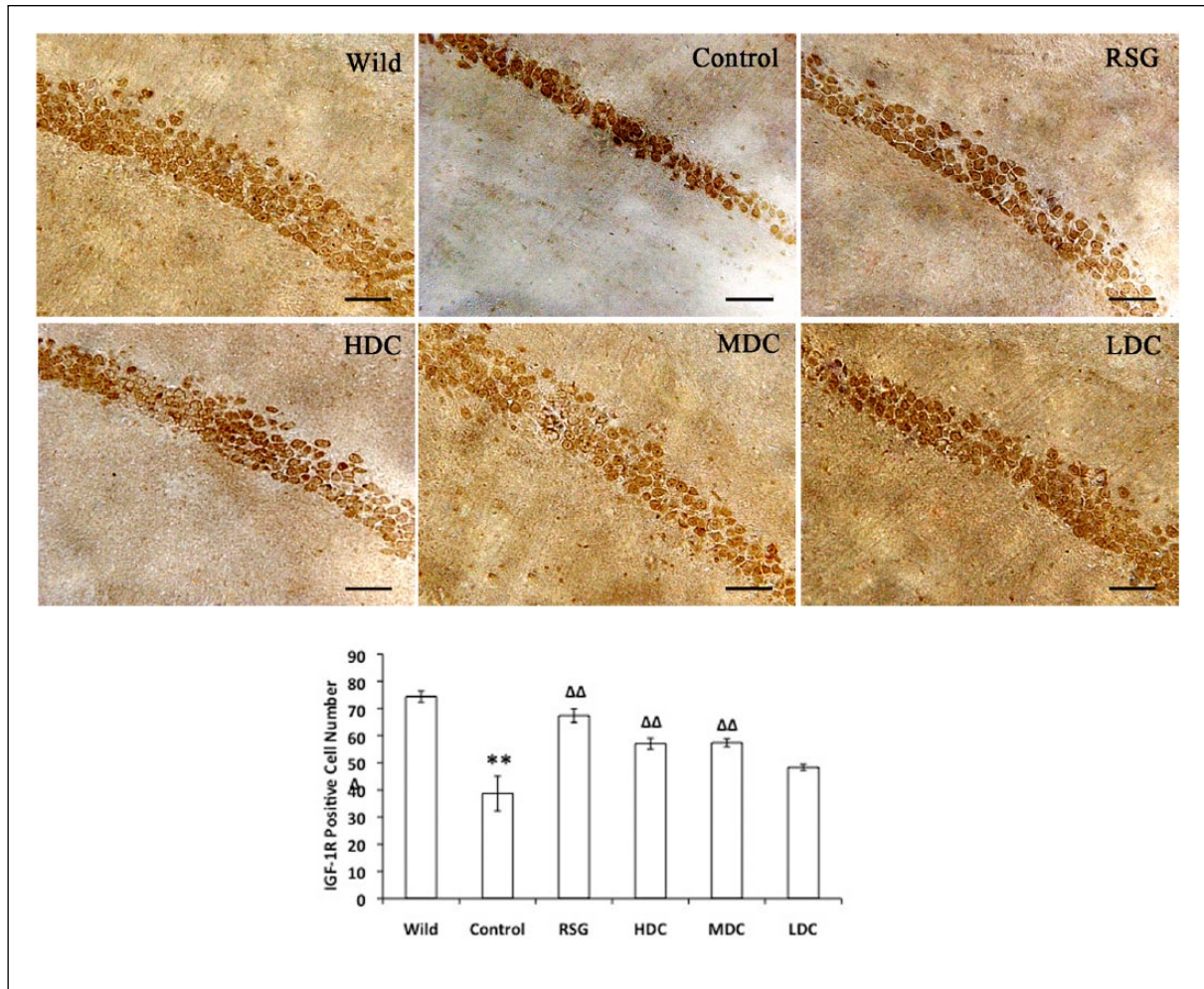


Figure 5. Effect of curcumin on IGF-1R expression in the hippocampal CA1 region. This figure shows IGF-1R expression in the hippocampal CA1 region using IHC analysis. Compared with the Control group, there are significantly more IGF-1R positive stained cells in the RSG, HDC and MDC groups ($P < 0.01$).

Effects of curcumin on IRS-1 expression in the hippocampal CA1 region

IHC staining of the hippocampal CA1 region showed that IRS-1 proteins were located primarily in the cytomembrane and cytoplasm. In the Wild group, IRS-1 positive neurons were only lightly stained and were distributed sparsely, primarily in the cytomembrane. In the Control group, the cytoplasm was strongly stained and the number of positively stained neurons was significantly higher compared with the Wild group ($P < 0.01$). In contrast to the Control group, IRS-1 positive neurons were more sparsely distributed and staining was lighter in all treatment groups. There were significantly ($P < 0.05$) fewer positively stained neurons in the LDC group than in the Control group. The difference was particularly significant ($P < 0.01$)

for the RSG positive control and the HDC and MDC treatment groups (Figure 6).

Western blot analysis showed that IRS-1 expression in the Control group was significantly higher than in the Wild group ($P < 0.01$). Compared with the Control group, IRS-1 protein expression was significantly lower in the RSG, MDC and HDC groups ($P < 0.01$ for RSG and MDC and $P < 0.05$ for HDC) as indicated by the thinner bands and paler staining (Figure 6).

Effects of curcumin on IRS-2 expression in the hippocampal CA1 region

IHC staining showed that, in contrast to the wild-type mice, the transgenic mice in the Control group had significantly less IRS-2 positive cells ($P < 0.01$). Compared with the Control group, there

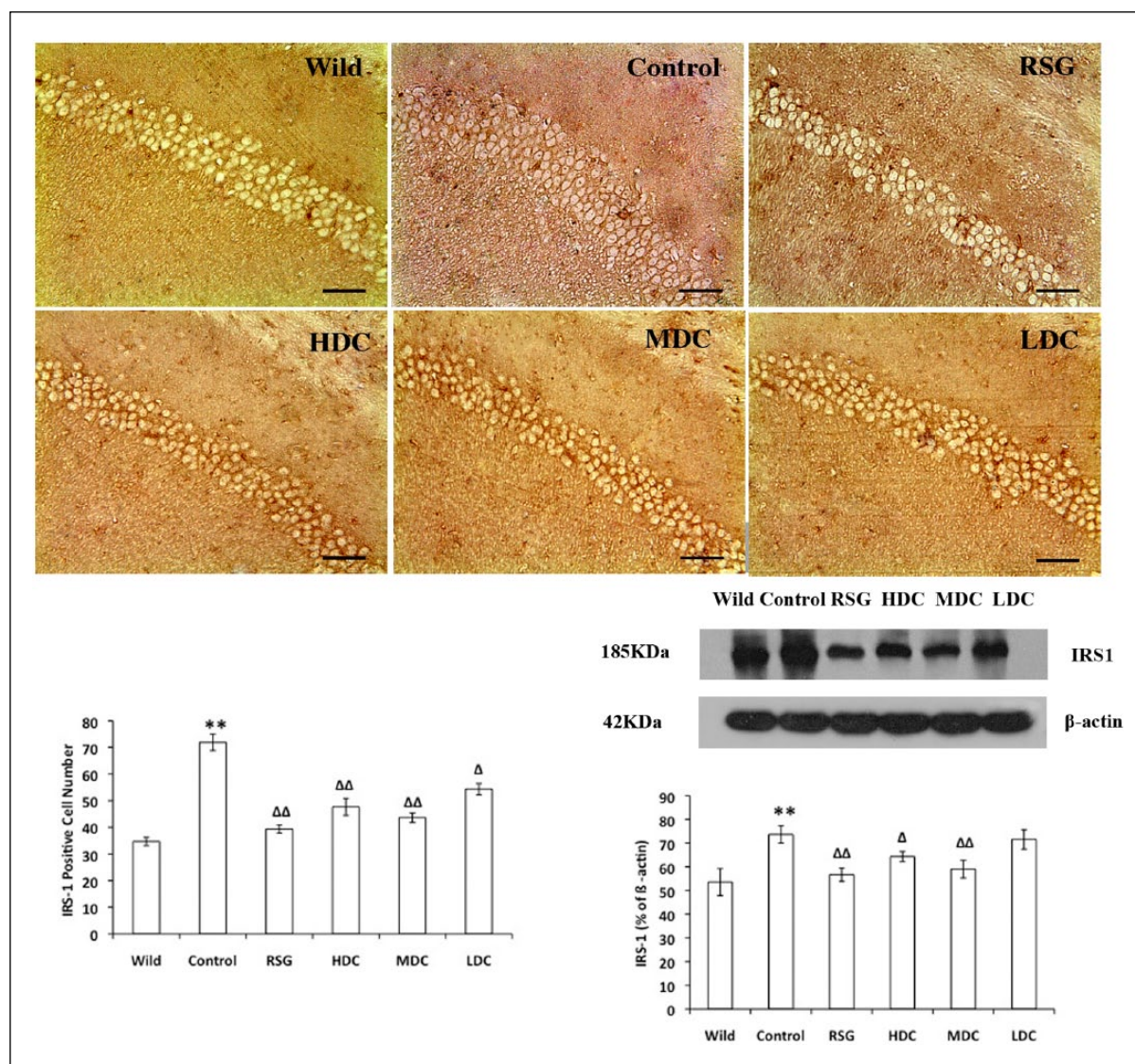


Figure 6. Effect of curcumin on IRS-1 expression in the hippocampal CA1 region. The IHC analysis indicated that there are significantly more IRS-1 positive cells in the treatment groups (RSG, HDC and MDC groups: $P < 0.01$; LDC: $P < 0.05$) than in the Control group. Western blot analysis showed that, compared with the Control group, the RSG, HDC and MDC treatment groups (RSG and MDC groups: $P < 0.01$; HDC: $P < 0.05$) showed significant increases in the number of IRS-1 proteins.

were significantly more IRS-2 positive cells in the mice in both the RSG and MDC groups ($P < 0.05$) (Figure 7).

Effects of curcumin on PI3K expression in the hippocampal CA1 region

Positive staining of PI3K was shown in cytoplasm and the cytomembrane, appearing as yellowy-brown stained particles in plasma. Positively stained neurons in the hippocampal CA1 region have big circular or oval-shaped cell bodies. Quantification showed that the number of PI3K

positive cells in the Control group was significantly lower than in the Wild group ($P < 0.05$). In contrast with the Control group, the numbers of PI3K positively stained cells in the RSG and MDC groups were significantly higher ($P < 0.05$). Treatment with high and low dose curcumin also showed an obvious increase, but was not statistically significant (Figure 8).

Western blot analysis of PI3K showed that there was less PI3K protein expression in the Control group than in the Wild group ($P < 0.01$). Compared with the Control group, RSG, HDC and MDC treatment significantly increased the amount of

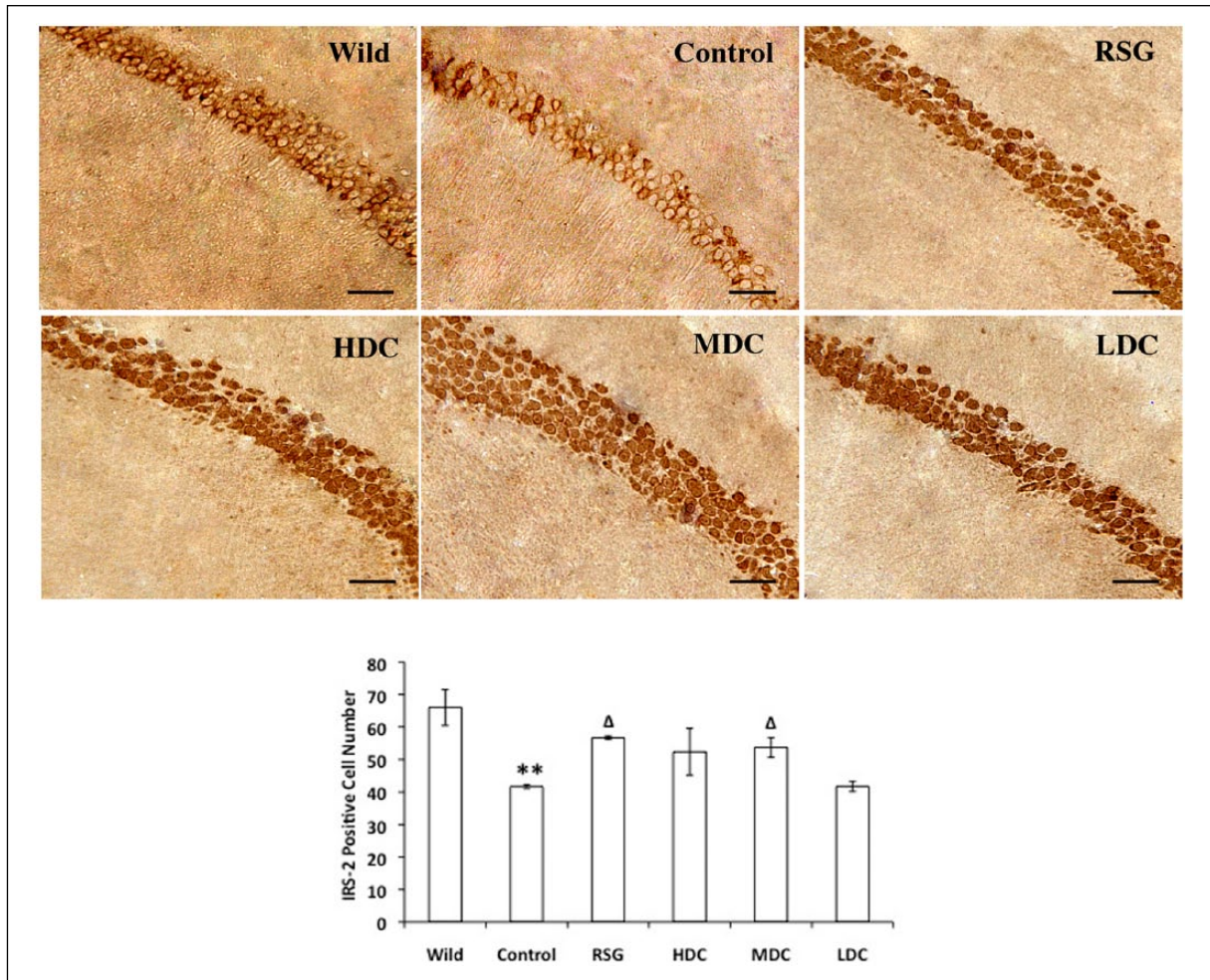


Figure 7. Effect of curcumin on IRS-2 expression in the hippocampal CA1 region. IHC staining of IRS-2 in the hippocampal CA1 region showed that, compared with the Control group, both the RSG and MDC groups showed a significant increase in IRS-2 expression ($P < 0.05$).

PI3K ($P < 0.01$ for RSG and MDC and $P < 0.05$ for HDC) (Figure 8).

Effects of curcumin on p-PI3K expression in the hippocampal CA1 region

IHC staining of p-PI3K showed that the number of p-PI3K positively stained neurons was significantly lower in the Control group than in the Wild group ($P < 0.01$). Compared with the Control group, all intervention groups showed a significant increase in the number of p-PI3K positive cells ($P < 0.05$) (Figure 9).

Similar results were found in the western blot analysis. The amount of p-PI3K protein in the Control group was significantly lower than in the wild-type mice ($P < 0.01$). RSG and MDC treatment significantly increased the amount p-PI3K protein compared with the Control group ($P < 0.01$).

The effect of HDC treatment was less significant ($P < 0.05$) and LDC treatment showed no statistical difference when compared with the Control group (Figure 9).

Effects of curcumin on AKT expression in the hippocampal CA1 region

IHC staining showed that there were less Akt positively stained cells in the Control group than in the Wild group ($P < 0.05$). In contrast to the Control group, the number of Akt positive cells in the RSG, HDC and MDC groups was significantly higher ($P < 0.05$) (Figure 10).

Western blot analysis showed that Akt protein expression in the Control group was significantly lower than in the Wild group ($P < 0.01$). In contrast to the Control group, the amount of Akt protein in

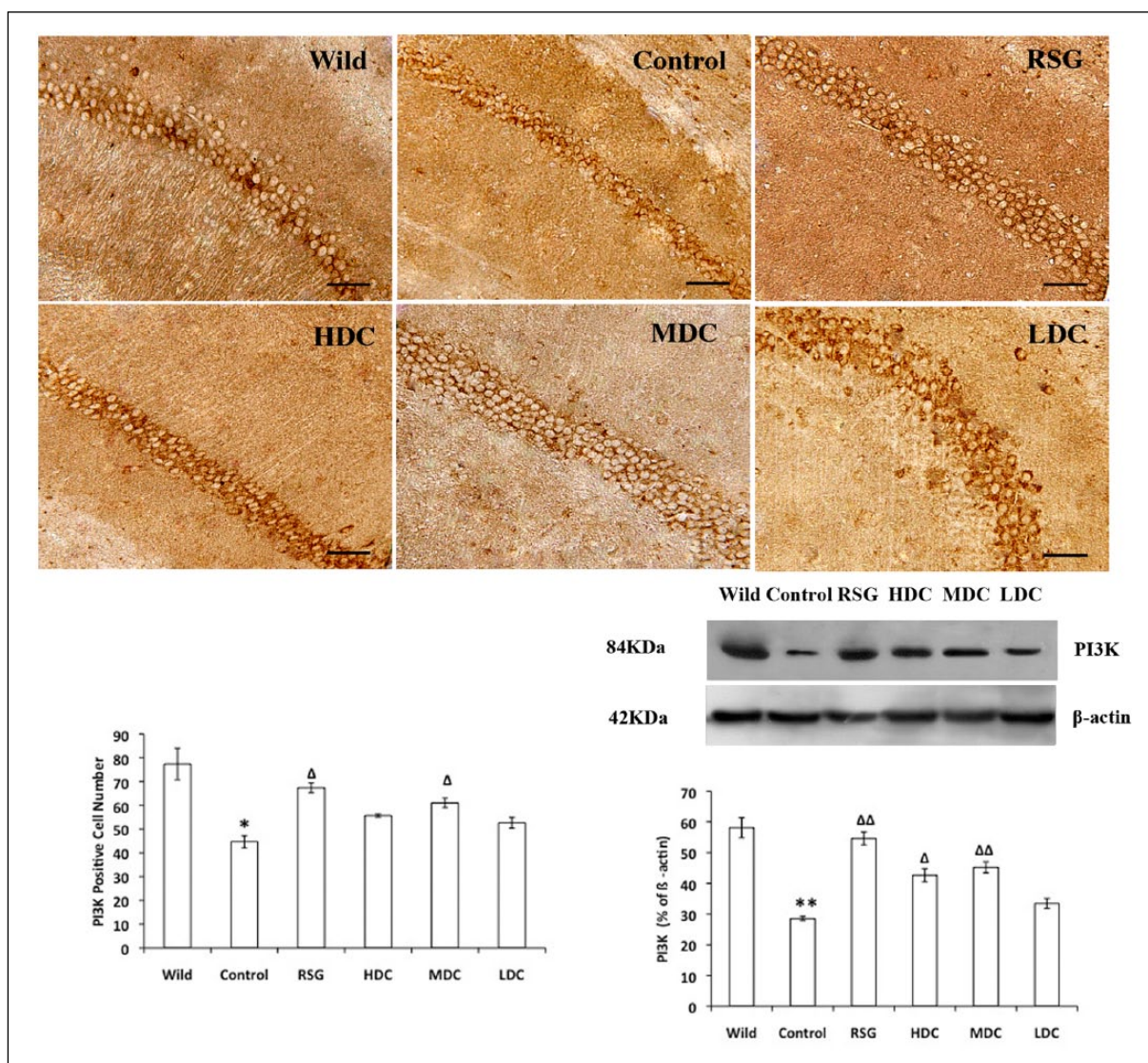


Figure 8. Effect of curcumin on PI3K expression in the hippocampal CA1 region. Compared with the vehicle treatment in the Control group, IHC analysis showed that RSG and MDC treatment significantly increased the number of PI3K positive cells ($P < 0.05$), while western blot analysis showed that RSG, HDC and MDC treatments significantly improved PI3K expression (HDC: $P < 0.05$; RSG and MDC: $P < 0.01$).

the RSG and MDC treatment groups was significantly higher ($P < 0.01$). The effect of HDC was less significant ($P < 0.05$) and LDC treatment showed no statistical difference when compared with the Control group (Figure 10).

Effects of curcumin on p-Akt expression in the hippocampal CA1 region

IHC staining showed that the number of p-Akt positive cells in the Control group was lower than in the Wild group ($P < 0.01$). In contrast to the Control group, there were more Akt positive cells in RSG, MDC and HDC groups ($P < 0.01$

for RSG and MDC and $P < 0.05$ for HDC) (Figure 11).

Western blot analysis showed that p-Akt protein expression in the Control group was significantly lower than in the Wild group ($P < 0.01$). In contrast to the Control group, p-Akt protein expression in the RSG, MDC and HDC groups was significantly higher ($P < 0.01$ for the RSG and MDC groups and $P < 0.05$ for the HDC group) (Figure 11).

Discussion

Glucose is the primary energy source for the brain. If this fuel is lacking, neurotransmitters are not

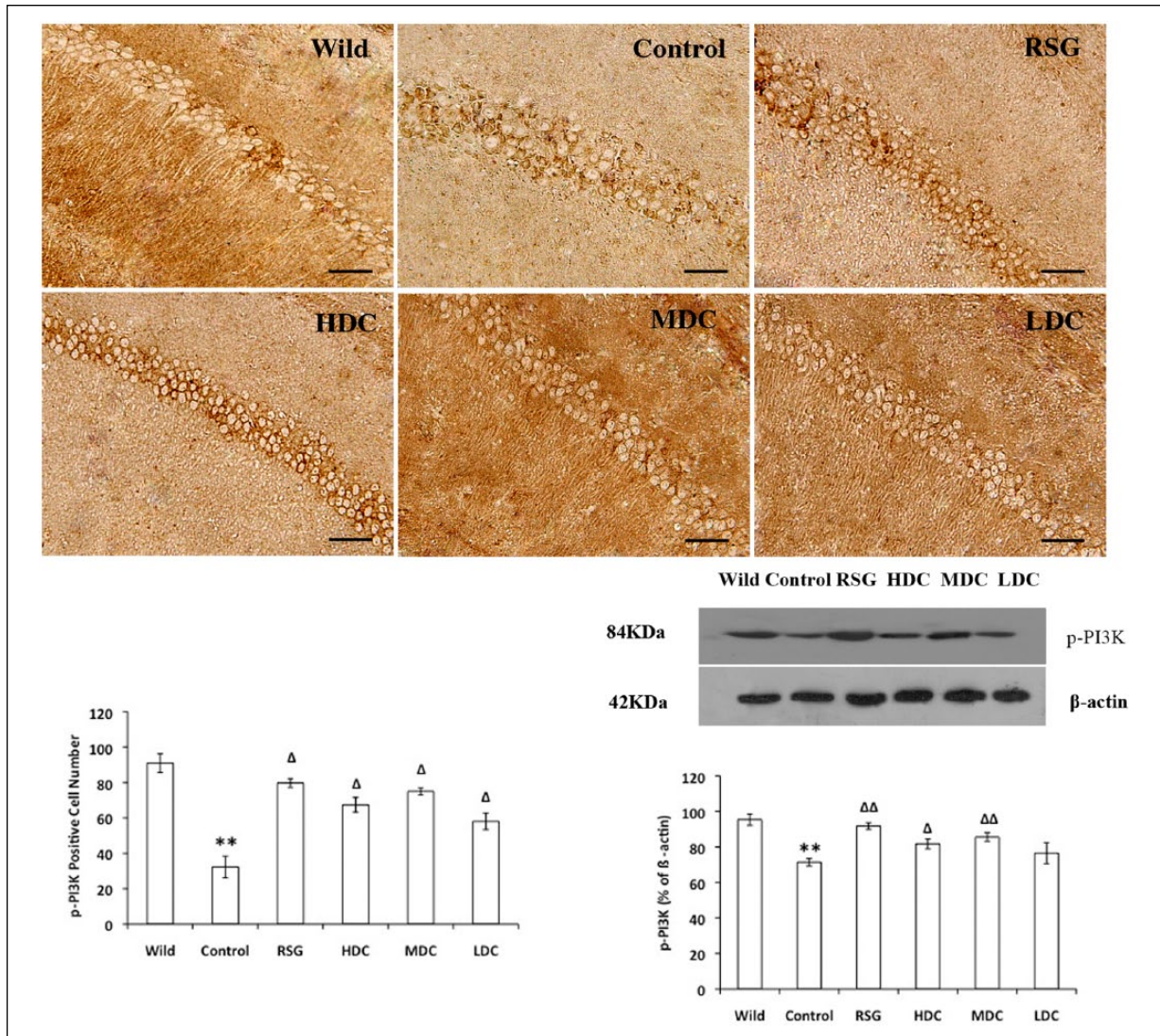


Figure 9. Effect of curcumin on p-PI3K expression in the hippocampal CA1 region. IHC analysis showed that all treatment groups significantly increased the numbers of p-PI3K positive cells compared with the Control group ($P < 0.05$). Western blot analysis showed that, compared with the Control group, RSG, HDC and MDC treatment groups showed significant increases in p-PI3K expression (HDC: $P < 0.05$; RSG and MDC: $P < 0.01$).

synthesised and communication between neurons breaks down. Numerous studies have shown that brain glucose transport and utilisation are impaired in elderly patients with AD.^{32–35} It is believed that the extent of glucose hypometabolism correlates with the severity of cognitive impairment.³⁶ Over the past two decades, PET has been adopted as a standard technique to quantify several processes to monitor cerebral health and function, including cerebral blood flow, cerebral blood volume and rate of cerebral glucose metabolism.³⁷ The majority of PET scans in the memory-impaired population use 18F-FDG as a radio-labelled tracer. A multi-centre study comprising ten PET centres

showed that the distinction between controls and AD patients had a 93% sensitivity and a 93% specificity.³⁸

In our study, using the micro-PET technique, we were able to show the mouse brain 18F-FDG intake conditions, which directly indicated the rate of glucose metabolism. The images showed that there were more 18F-FDG accumulations in the Wild and MDC treatment groups than in the Control group. Quantification results confirmed that the whole brain 18F-FDG intake rate was greater in the Wild and MDC groups than in the Control group. Studies have shown that the metabolism of cerebral glucose was impaired in

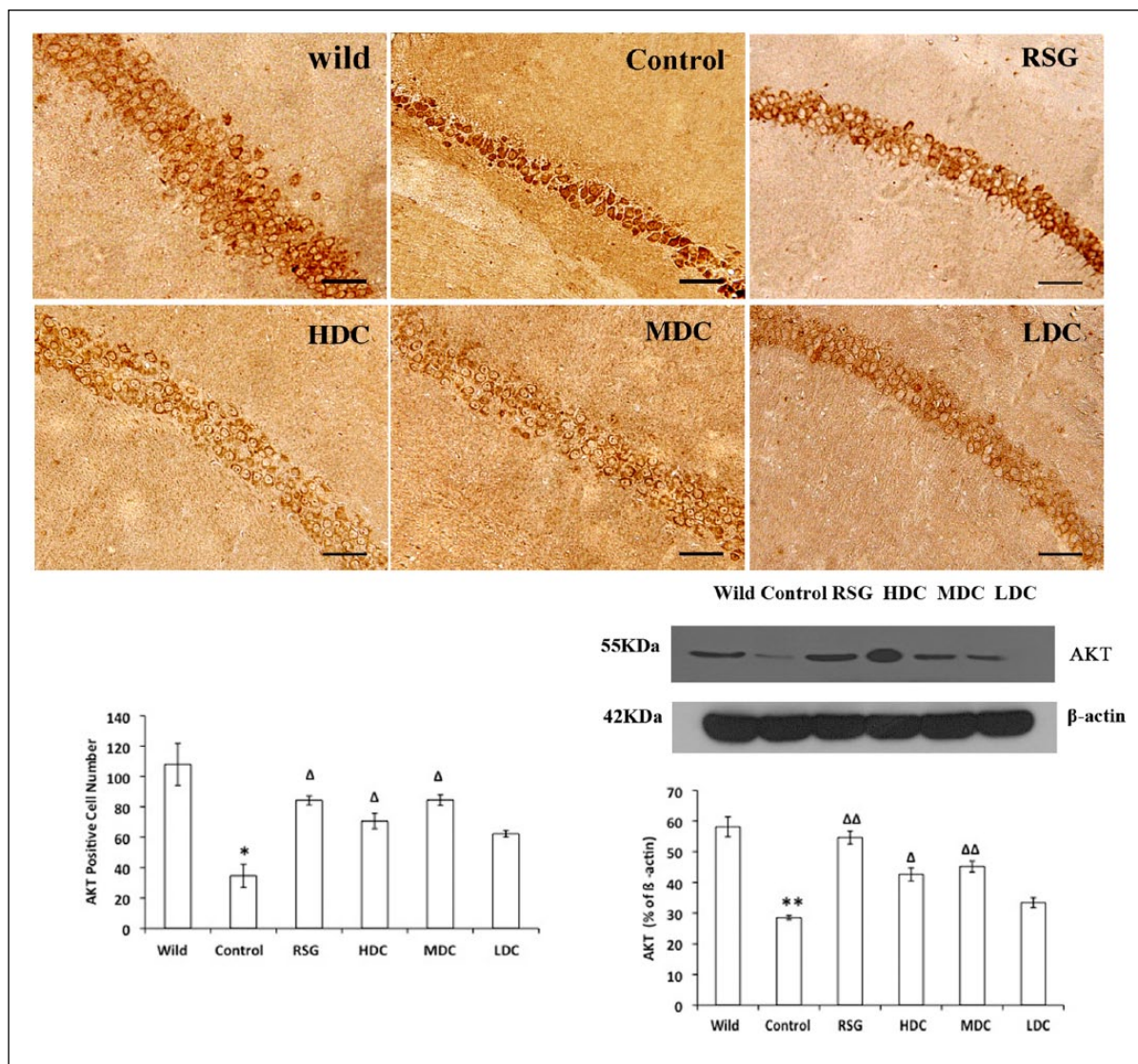


Figure 10. Effect of curcumin on Akt expression in the hippocampal CA1 region. Compared with the Control group, IHC staining showed a significant increase ($P < 0.05$) in Akt expression in RSG, HDC and MDC treatment groups. Western blot analysis also revealed a significant increase in Akt expression in the RSG, HDC and MDC treatment groups (HDC: $P < 0.05$; RSG and MDC: $P < 0.01$).

the neocortical-associated areas of the brain (including the posterior cingulate, temporoparietal and frontalmultimodal cortex), whereas the primary visual and sensorimotor cortex, basal ganglia and cerebellum are relatively well preserved.³⁹ Based on this information, we investigated the frontal and temporal lobe areas which are related to memory and learning functions. The quantification results showed that rate of glucose metabolism was higher in the Wild and MDC groups than in the Control group. The PET analysis concluded that three months of curcumin treatment improves cerebral glucose intake and energy metabolism in APP/PS1 mice.

Despite the crucial role glucose plays in brain function, brain neurons are unable to generate and store glucose; therefore, glucose must be supplied continuously from the peripheral system. Glucose travels via GLUTs from blood to brain through the blood-brain barrier (BBB).⁴⁰ The GLUT family is made up of a large group of membrane proteins, which employ a saturation mechanism to facilitate the transportation of glucose from areas where it is highly concentrated to areas where it is less concentrated, and which does not consume energy during the transfer. Based on their sequence similarities, the GLUT family has been divided into three different classes. Some isoforms, such as

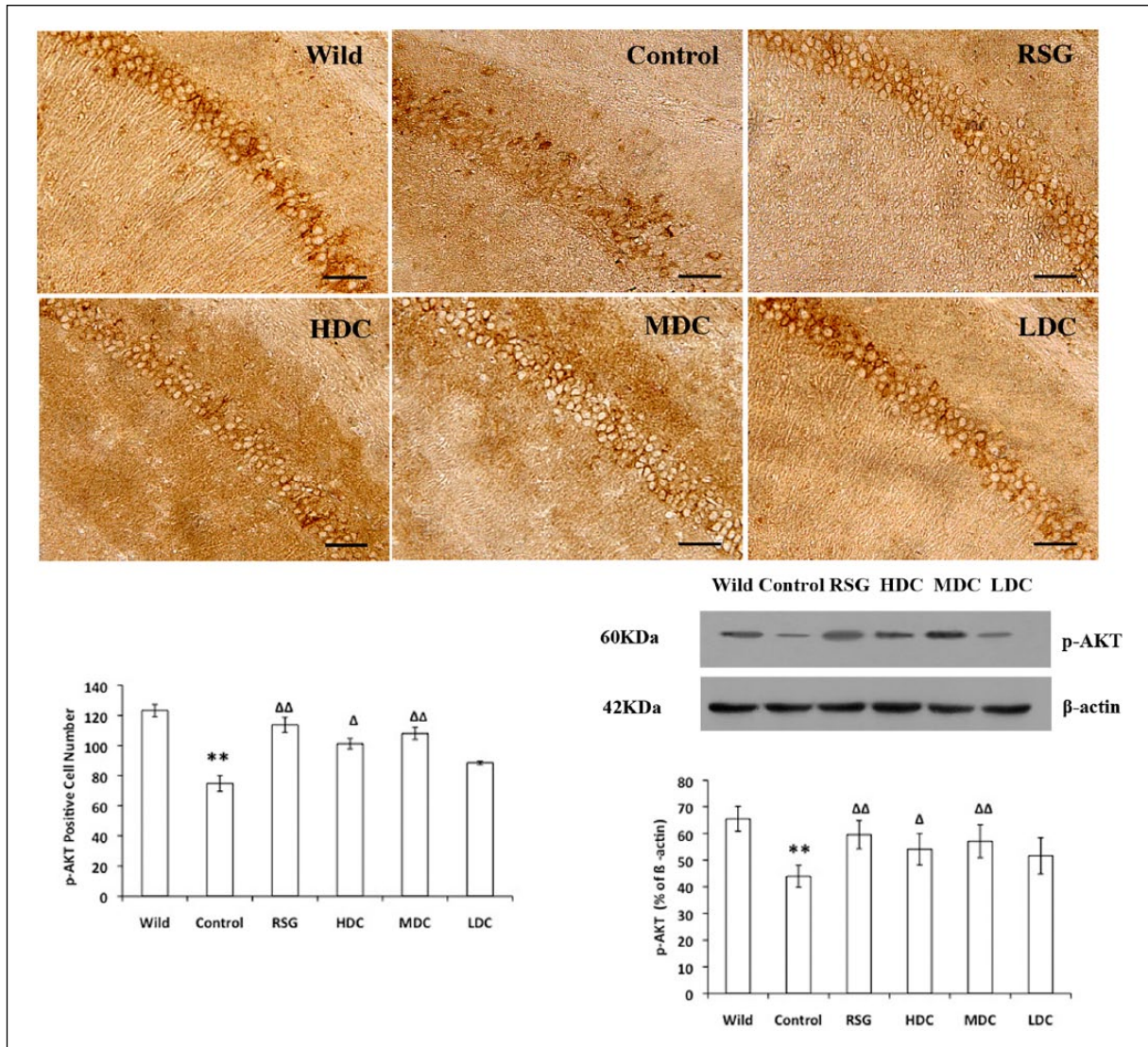


Figure 11. Effect of curcumin on p-Akt expression in the hippocampal CA1 region. In both the IHC and western blot analysis, RSG, HDC and MDC treatment resulted in significant increases in p-Akt expression ($P < 0.05$ for HDC and $P < 0.01$ for RSG and MDC, respectively) compared with the Control group.

GLUT1 and GLUT3, are widely expressed in the central nervous system and appear to be responsible for the majority of glucose uptake and utilisation in brain.^{41,42} GLUT1 was the first glucose transporter identified in the brain and is expressed on BBB endothelial cells and cortical membranes.⁴³ GLUT1 represents the passageway for glucose into the brain and regulates the availability of metabolic fuels to the neurons.⁴⁴ Because GLUT3 isoforms are expressed on neurons, GLUT3 is also referred to as the neuron-specific glucose transporter.⁴² The transportation of glucose from blood to brain requires coordination from all participants, including endothelial cells,

glia (especially astrocytes) and neurons. The uptake of glucose by neurons was mediated by GLUT3.⁴⁵ Decreased concentrations of GLUT1 and GLUT3 were also found in the brains of patients with AD.^{34,46,47} Under normal physiological conditions, glucose transportation through the BBB is not the determining factor in the rate of glucose utilisation in brains,⁴⁸ however, under pathological conditions when GLUT1 and GLUT3 expression are impaired, an insufficient supply of glucose will lead to metabolic impairments.⁴⁸

In this study, using IHC staining and western blot analysis, we showed that treatment with a medium dose of curcumin was able to consistently and

significantly improve GLUT1 and GLUT3 protein expression ($P < 0.05$) compared with the Control group. This may explain the high rate of cerebral glucose metabolism we found in the brains of the AD mice treated with medium dose curcumin.

It is well known that in peripheral tissue, insulin resistance is a feature of type 2 diabetes. Recent studies have demonstrated that insulin resistance also exists in the AD brain.^{6,49} Binding of insulin and/or IGF-1 to insulin and IGF-1 receptors respectively induces a conformational change of these tyrosine kinase receptors and promotes receptor autophosphorylation, thereby recruiting docking proteins including IRS to the cell membrane. Thereafter, IRS/PI3K/Akt signal cascades are activated.⁵⁰ Reduced response to IGF-1/insulin leads to the formation of degenerative neurons,⁵¹ A β accumulation and tau phosphorylation,⁵² and increases the risk of AD.^{6,51} Treatment with insulin, however, can improve memory function in both humans and experimental animals.⁵³

The IRS family of docking proteins is composed of six proteins, IRS-1 to IRS-6. Of these family members, IRS-1 and IRS-2 are responsible for most of the pleiotropic effects of insulin and IGF-1.⁵⁴ IRS molecules are key mediators of insulin signal transduction and play an important role in maintaining basic cell functions such as growth, survival and metabolism. IRS-1 and IRS-2 are the two main substrates of insulin receptor tyrosine kinase and IGF receptor kinase and most of the generation or regulation of insulin signalling is through IRS-1, IRS-2 or their homologues. Cell and transgenic mice experiments have indicated that the mechanism of insulin response is through the tyrosine and serine phosphorylation of IRS-1 and IRS-2 in conjunction with regulating hormones and inflammatory cytokines.^{55–57}

In our previous study using curcumin in an AD mouse model, we found that curcumin-treated mice showed significant memory improvement as demonstrated in the water maze behaviour test.²² Given the established correlation between insulin resistance and AD, we hypothesised that the curcumin-mediated cognition improvement may have been the result of ameliorating the impaired insulin signalling in the IR/IRS-1/PI3K/Akt and IGF-1R/IRS-2/PI3K/Akt pathways. This study is a continuation of our previous one.²² We used the tissues from the same group of mice which were examined in our 2014 publication investigating A β deposition

and cognition. In this study, however, we used western blot and IHC staining methods to examine the major factors in the insulin/IGF-1 signalling pathway, including IR, IGF-1R, IRS, PI3K and Akt.

Our results showed increased basal levels of IR and IRS-1 and decreased basal levels of IGF-1R and IRS-2, in conjunction with reduced downstream PI3K/Akt expression, in the transgenic AD mice compared with the wild-type mice. We found that curcumin treatment can ameliorate the impaired insulin signalling pathway by upregulating IGF-1R, IRS-2, PI3K, p-PI3K and Akt protein expression. IR, as demonstrated in both the IHC staining and western blot testing, was downregulated by curcumin. Of the three dosages tested, the medium dose of curcumin proved to be the optimal dose as all tests showed a significant difference between medium curcumin treatment and vehicle treatment.

Conflicting findings have been reported regarding levels of IR in AD brains. In 2005, Steen found that IR gene expression was strikingly reduced in AD;⁵⁸ using western blot analysis, Liu et al. showed that IR beta unit was reduced in an AD brain sample.⁵⁹ However, Zhao et al. found no changes in total IR levels in total homogenates from ADDL-treated neurons as measured by western blots; further study revealed no change to intracellular IR levels in ADDL-treated neurons, but did find a rapid and substantial loss of neuronal surface IRs—specifically on dendrites bound by ADDLs—and increased receptor immunoreactivity in the cell body.^{23,60} The finding that synapse vulnerability to ADDLs is mitigated by insulin suggests that bolstering brain insulin signaling, which declines with aging and diabetes, could have significant potential to slow or deter AD pathogenesis.⁶⁰ In our study, IHC staining and western blot testing both showed that IR was increased in AD mice compared with wild-type mice. We further analysed IR mRNA using RT-PCR methodology and the results showed increased levels of IR mRNA in AD mice, which supports our findings (unpublished data). Receptor distribution is an important function; future study focusing on IR distribution might explain the discrepancy.

As a neuroprotective drug, curcumin is well known for its anti-inflammatory and antioxidant effects as well as its ability to reduce plaque deposition in central nervous system (CNS) and AD models.^{61–64} That dietary treatment with fish oil/DHA, curcumin or a combination of both has the potential

to improve insulin/trophic signaling and cognitive deficits in AD.⁶⁵ Emerging data have shown that brain insulin resistance is associated with the abnormal glucose metabolism in AD.⁶⁶ Our current study showed that curcumin can promote brain glucose metabolism and ameliorate insulin signalling pathways in AD mice. Our previous study demonstrated that curcumin reduces A β 40, A β 42 and A β -derived diffusible ligands in the mouse hippocampus, and improving learning and memory. The present study provides additional evidence of the potential efficacy of curcumin therapy in AD.

Acknowledgements

The authors thank Mrs. Ann Kolkin for her helpful suggestions and critical editorial review.

Declaration of conflicting interests

The author(s) declared no potential conflicts of interest with respect to the research, authorship, and/or publication of this article.

Funding

This study was supported by the National Natural Science Foundation of China (no. 81073076) and (no. 81573927), the scientific research and graduate training project of Beijing municipal commission of education (2016).

References

1. Armstrong RA (2009) The molecular biology of senile plaques and neurofibrillary tangles in Alzheimer's disease. *Folia Neuropathologica* 47: 289–299.
2. Goedert M and Spillantini MG (2006) A century of Alzheimer's disease. *Science* 314: 777–781.
3. Selkoe DJ (1991) The molecular pathology of Alzheimer's disease. *Neuron* 6: 487–498.
4. Hardy JA and Higgins GA (1992) Alzheimer's disease: The amyloid cascade hypothesis. *Science* 256: 184–185.
5. Kaidanovich-Beilin O, Cha DS and McIntyre RS (2012) Crosstalk between metabolic and neuropsychiatric disorders. *F1000 Biology Reports* 4: 14.
6. Talbot K, Wang HY, Kazi H, et al. (2012) Demonstrated brain insulin resistance in Alzheimer's disease patients is associated with IGF-1 resistance, IRS-1 dysregulation, and cognitive decline. *Journal of Clinical Investigation* 122: 1316–1338.
7. Miles WR and Root HF (1922) Psychologic tests applied in diabetic patients. *Archives of Internal Medicine* 30:767–777.
8. de la Torre JC (2008) Pathophysiology of neuronal energy crisis in Alzheimer's disease. *Neurodegenerative Diseases* 5: 126–132.
9. Lane RF, Shineman DW, Steele JW, et al. (2012) Beyond amyloid: The future of therapeutics for Alzheimer's disease. *Advances in Pharmacology* 64: 213–271.
10. Hooijmans CR, Graven C, Dederen PJ, et al. (2007) Amyloid beta deposition is related to decreased glucose transporter-1 levels and hippocampal atrophy in brains of aged APP/PS1 mice. *Brain Research* 1181: 93–103.
11. Cole SL, Grudzien A, Manhart IO, et al. (2005) Statins cause intracellular accumulation of amyloid precursor protein, beta-secretase-cleaved fragments, and amyloid beta-peptide via an isoprenoid-dependent mechanism. *Journal of Biological Chemistry* 280: 18755–18770.
12. Nelson TJ and Alkon DL (2005) Insulin and cholesterol pathways in neuronal function, memory and neurodegeneration. *Biochemical Society Transactions* 33: 1033–1036.
13. de la Monte SM and Wands JR (2005) Review of insulin and insulin-like growth factor expression, signaling, and malfunction in the central nervous system: Relevance to Alzheimer's disease. *Journal of Alzheimers Disease* 7: 45–61.
14. Long-Smith CM, Manning S, McClean PL, et al. (2013) The diabetes drug liraglutide ameliorates aberrant insulin receptor localisation and signalling in parallel with decreasing both amyloid- β plaque and glial pathology in a mouse model of Alzheimer's disease. *Neuromolecular Medicine* 15: 102–114.
15. Aggarwal BB, Sundaram C, Malani N, et al. (2007) Curcumin: The Indian solid gold. *Advances in Experimental Medicine and Biology* 595: 1–75.
16. Darvesh AS, Carroll RT, Bishayee A, et al. (2012) Curcumin and neurodegenerative diseases: A perspective. *Expert Opinion on Investigative Drugs* 21: 1123–1140.
17. Marathe SA, Dasgupta I, Gnanadhas DP, et al. (2011) Multifaceted roles of curcumin: two sides of a coin! *Expert Opinion on Biological Therapy* 11: 1485–1499.
18. Ahmed T, Enam SA and Gilani AH (2010) Curcuminoids enhance memory in an amyloid-infused rat model of Alzheimer's disease. *Neuroscience* 169: 1296–1306.
19. Ahmed T, Gilani AH, Hosseinmardi N, et al. (2011) Curcuminoids rescue long-term potentiation impaired by amyloid peptide in rat hippocampal slices. *Synapse* 65: 572–582.
20. Garcia-Alloza M, Borrelli LA, Rozkalne A, et al. (2007) Curcumin labels amyloid pathology in vivo, disrupts existing plaques, and partially restores distorted neurites in an Alzheimer mouse model. *Journal of Neurochemistry* 102: 1095–1104.
21. Maiti P, Hall TC, Paladugu L, et al. (2016) A comparative study of dietary curcumin, nanocurcumin,

- and other classical amyloid-binding dyes for labeling and imaging of amyloid plaques in brain tissue of 5 \times -familial Alzheimer's disease mice. *Histochem Cell Biol* 146: 609–625.
22. Wang P, Su C, Li R, et al. (2014) Mechanisms and effects of curcumin on spatial learning and memory improvement in APP^{swe}/PS1^{dE9} Mice. *Journal of Neuroscience Research* 92: 218–231.
 23. Zhao WQ, De Felice FG, Fernandez S, et al. (2008) Amyloid beta oligomers induce impairment of neuronal insulin receptors. *FASEB Journal* 22: 246–260.
 24. Gong Y, Chang L, Viola KL, et al. (2003) Alzheimer's disease-affected brain: Presence of oligomeric A beta ligands (ADDLs) suggests a molecular basis for reversible memory loss. *Proceedings of the National Academy of Sciences of the United States of America* 100: 10417–10422.
 25. Taniguchi CM, Emanuelli B and Kahn CR (2006) Critical nodes in signalling pathways: insights into insulin action. *Nature Reviews. Molecular and Cellular Biology* 7: 85–96.
 26. Akomolafe A, Beiser A, Meigs JB, et al. (2006) Diabetes mellitus and risk of developing Alzheimer disease: Results from the Framingham Study. *Archives of Neurology* 63: 1551–1555.
 27. Watson GS and Craft S (2003) The role of insulin resistance in the pathogenesis of Alzheimer's disease: implications for treatment. *CNS Drugs* 17: 27–45.
 28. Watson GS, Cholerton BA, Reger MA, et al. (2005) Preserved cognition in patients with early Alzheimer disease and amnesic mild cognitive impairment during treatment with rosiglitazone: A preliminary study. *American Journal of Geriatric Psychiatry* 13: 950–958.
 29. Wang P, Jiang S, Cui Y, et al. (2011) The n-terminal 5-MER peptide analogue P165 of amyloid precursor protein exerts protective effects on SH-SY5Y cells and rat hippocampus neuronal synapses. *Neuroscience* 173: 169–178.
 30. Zhao YL, Ma XB and Han WD (2006) *Basic laboratory techniques in molecular biology*. Beijing: Qinghua University Publishing House.
 31. Lyck L, Jelsing J, Jensen PS, et al. (2006) Immunohistochemical visualization of neurons and specific glial cells for stereological application in the porcine neocortex. *Journal of Neuroscience Methods* 152: 229–242.
 32. Benson DF, Kuhl DE, Hawkins RA, et al. (1983) The fluorodeoxyglucose 18F scan in Alzheimer's disease and multi-infarct dementia. *Archives of Neurology* 40: 711–714.
 33. Friedland RP, Jagust WJ, Huesman RH, et al. (1989) Regional cerebral glucose transport and utilization in Alzheimer's disease. *Neurology* 39: 1427–1434.
 34. Harr SD, Simonian NA and Hyman BT (1995) Functional alterations in Alzheimer's disease: Decreased glucose transporter 3 immunoreactivity in the perforant pathway terminal zone. *Journal of Neuropathology and Experimental Neurology* 54: 38–41.
 35. Piert M, Koeppe RA, Giordani B, et al. (1996) Diminished glucose transport and phosphorylation in Alzheimer's disease determined by dynamic FDG-PET. *Journal of Nuclear Medicine* 37: 201–208.
 36. Schaller BJ (2008) Strategies for molecular imaging dementia and neurodegenerative diseases. *Neuropsychiatric Disease and Treatment* 4: 585–612.
 37. Silverman DH and Alavi A (2005) PET imaging in the assessment of normal and impaired cognitive function. *Radiology Clinics of North America* 43: 67–77, x.
 38. Heiss WD and Zimmermann-Meinzingen S (2012) PET imaging in the differential diagnosis of vascular dementia. *Journal of Neurological Science* 322: 268–273.
 39. Herholz K (2003) PET studies in dementia. *Annals of Nuclear Medicine* 17: 79–89.
 40. Maher F, Vannucci SJ and Simpson IA (1994) Glucose transporter proteins in brain. *FASEB Journal* 8: 1003–1011.
 41. Duelli R and Kuschinsky W (2001) Brain glucose transporters: Relationship to local energy demand. *News in Physiological Sciences* 16: 71–76.
 42. McEwen BS and Reagan LP (2004) Glucose transporter expression in the central nervous system: Relationship to synaptic function. *European Journal of Pharmacology* 490: 13–24.
 43. Ahmad W (2013) Overlapped metabolic and therapeutic links between Alzheimer and diabetes. *Molecular Neurobiology* 47: 399–424.
 44. Giaume C, Taberero A and Medina JM (1997) Metabolic trafficking through astrocytic gap junctions. *Glia* 21: 114–123.
 45. Dwyer DS, Vannucci SJ and Simpson IA (2002) Expression, regulation, and functional role of glucose transporters (GLUTs) in brain. *International Review of Neurobiology* 51: 159–188.
 46. Mooradian AD, Chung HC and Shah GN (1997) GLUT-1 expression in the cerebra of patients with Alzheimer's disease. *Neurobiology of Aging* 18: 469–474.
 47. Simpson IA, Chundu KR, Davies-Hill T, et al. (1994) Decreased concentrations of GLUT1 and GLUT3 glucose transporters in the brains of patients with Alzheimer's disease. *Annals of Neurology* 35: 546–551.
 48. Liu Y, Liu F, Iqbal K, et al. (2008) Decreased glucose transporters correlate to abnormal hyperphosphorylation of tau in Alzheimer disease. *FEBS Letters* 582: 359–364.
 49. Bomfim TR, Fornyy-Germano L, Sathler LB, et al. (2012) An anti-diabetes agent protects the mouse brain from defective insulin signaling caused by

- Alzheimer's disease-associated A β oligomers. *Journal of Clinical Investigation* 122: 1339–1353.
50. Candeias E, Duarte AI, Carvalho C, et al. (2012) The impairment of insulin signaling in Alzheimer's disease. *IUBMB Life* 64: 951–957.
 51. Moloney AM, Griffin RJ, Timmons S, et al. (2010) Defects in IGF-1 receptor, insulin receptor and IRS-1/2 in Alzheimer's disease indicate possible resistance to IGF-1 and insulin signalling. *Neurobiology of Aging* 31: 224–243.
 52. Killick R, Scales G, Leroy K, et al. (2009) Deletion of Irs2 reduces amyloid deposition and rescues behavioural deficits in APP transgenic mice. *Biochemical and Biophysical Research Communications* 386: 257–262.
 53. Huang CC, Lee CC and Hsu KS (2010) The role of insulin receptor signaling in synaptic plasticity and cognitive function. *Chang Gung Medical Journal* 33: 115–125.
 54. Ghasemi R, Haeri A, Dargahi L, et al. (2013) Insulin in the brain: Sources, localization and functions. *Molecular Neurobiology* 47: 145–171.
 55. Hennige AM, Burks DJ, Ozcan U, et al. (2003) Upregulation of insulin receptor substrate-2 in pancreatic beta cells prevents diabetes. *Journal of Clinical Investigation* 112: 1521–1532.
 56. Kubota N, Tobe K, Terauchi Y, et al. (2000) Disruption of insulin receptor substrate 2 causes type 2 diabetes because of liver insulin resistance and lack of compensatory beta-cell hyperplasia. *Diabetes* 49: 1880–1889.
 57. Previs SF, Withers DJ, Ren JM, et al. (2000) Contrasting effects of IRS-1 vs IRS-2 gene disruption on carbohydrate and lipid metabolism in vivo. *Journal of Biological Chemistry* 275: 38990–38994.
 58. Steen E, Terry BM, Rivera EJ, et al. (2005) Impaired insulin and insulin-like growth factor expression and signaling mechanisms in Alzheimer's disease—is this type 3 diabetes? *Journal of Alzheimer's Disease* 7: 63–80.
 59. Liu Y, Liu F, Grundke-Iqbal I, et al. (2011) Deficient brain insulin signalling pathway in Alzheimer's disease and diabetes. *Journal of Pathology* 225: 54–62.
 60. De Felice FG, Vieira MNN, Bomfim TR, et al. (2009) Protection of synapses against Alzheimer's-linked toxins: Insulin signaling prevents the pathogenic binding of A β oligomers. *Proceedings of the National Academy of Sciences of the United States of America* 106: 1971–1976.
 61. Cole GM (2003) Ironic fate: Can a banned drug control metal heavies in neurodegenerative diseases? *Neuron* 37: 889–890.
 62. Frautschy SA, Hu W, Kim P, et al. (2001) Phenolic anti-inflammatory antioxidant reversal of A β -induced cognitive deficits and neuropathology. *Neurobiology of Aging* 22: 993–1005.
 63. Cole GM and Frautschy SA (2007) The role of insulin and neurotrophic factor signaling in brain aging and Alzheimer's Disease. *Experimental Gerontology* 42: 10–21.
 64. Begum AN, Jones MR, Lim GP, et al. (2008) Curcumin structure-function, bioavailability, and efficacy in models of neuroinflammation and Alzheimer's disease. *Journal of Pharmacology and Experimental Therapeutics* 326: 196–208.
 65. Ma QL, Yang F, Rosario ER, et al. (2009) Beta-amyloid oligomers induce phosphorylation of tau and inactivation of insulin receptor substrate via c-Jun N-terminal kinase signaling: Suppression by omega-3 fatty acids and curcumin. *Journal of Neuroscience* 29: 9078–9089.
 66. Umegaki H (2014) Type 2 diabetes as a risk factor for cognitive impairment: Current insights. *Clinical Interventions in Aging* 9: 1011–1019.